Self-Supervised Partial Cycle-Consistency for Multi-View Matching

Fedor Taggenbrock[1,2][0009−0002−6166−0865], Gertjan Burghouts[2][0000−0001−6265−7276], and Ronald Poppe[1][0000−0002−0843−7878]

[1] Utrecht University, Utrecht, Netherlands
[2] TNO, The Hague, Netherlands

Abstract. Matching objects across partially overlapping camera views is crucial in multi-camera systems and requires a view-invariant feature extraction network. Training such a network with cycle-consistency circumvents the need for labor-intensive labeling. In this paper, we extend the mathematical formulation of cycle-consistency to handle partial overlap. We then derive several cycle variants and introduce a pseudo-mask which directs the training loss to take partial cycle-consistency into account, consequently improving the self-supervised learning signal. We additionally present a time-divergent scene sampling scheme that improves the data input for self-supervised settings. Cross-camera matching experiments on the challenging DIVOTrack dataset show the merits of our approach. Compared to the self-supervised state-of-the-art, we achieve a 4.3 percentage point higher F1 score with our combined contributions. Our improvements are robust to reduced overlap in the training data, with substantial improvements in challenging scenes characterized by few matches between many people. Self-supervised feature networks trained with our method are effective at matching objects in a range of multi-camera settings, providing opportunities for complex tasks like large-scale multi-camera scene understanding.

Keywords: Self-Supervision · Multi-Camera · Feature Learning · Cycle-Consistency · Cross-View Multi-Object Tracking

1 Introduction

Matching people and objects across cameras is essential for multi-camera understanding [9,14,24]. Matches are commonly obtained by solving a multi-view matching problem. One crucial factor that determines the quality of the matching is the feature extractors' generalization to varying appearances as a result of expressiveness and view angle [15]. Feature extractors can be trained in a supervised setting, which requires labor-intensive data labeling [9]. The lack or scarcity of labeled data for novel domains is a limiting factor. Self-supervised techniques thus offer an attractive alternative because they can be trained directly on object and person bounding boxes, without the need of manual labeling.

Effective, view-invariant feature networks have been learned with self-supervision through cycle-consistency, for use in multi-view matching, cross-view multi-object tracking, and re-identification (Re-ID) [7,20]. Training these networks

only requires sets of objects where there is a sufficient amount of overlap between sets of objects between views. For multi-person matching and tracking, sets are typically detections of people from multiple camera views [7,9]. When the overlapping field of view between cameras decreases in the training data, self-supervised cycle-consistency methods have a diluted learning signal.

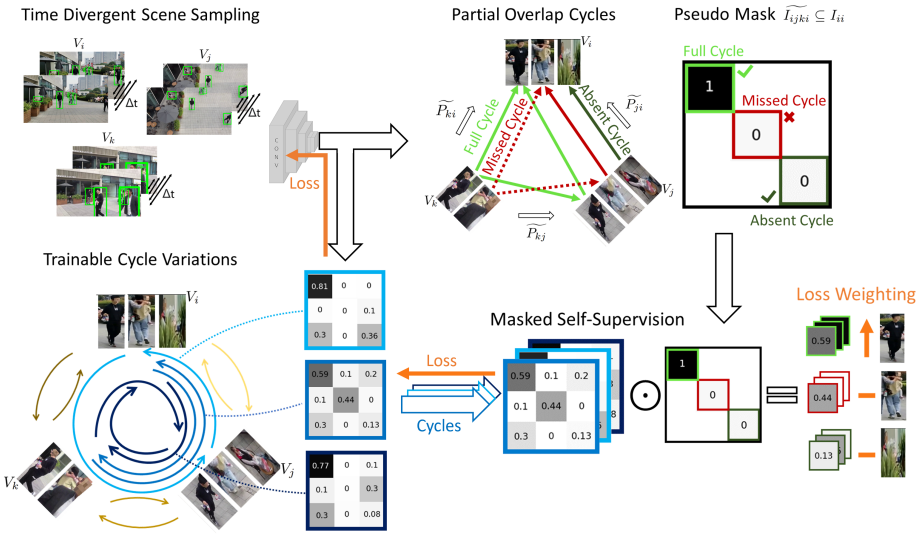

Fig. 1: Overview of our self-supervised cycle-consistency training method. Trainable cycle variations (left bottom) are constructed from sampled batches (left top). Cycle matrices represent chains of matches starting and ending in the same view. With partial overlap, however, we construct a pseudo-mask of the identity matrix (top right) to determine which specific cycles should be trained due to partial overlap. This pseudo-mask is then used to provide a weighted loss signal with more emphasis on the positive predicted cycles (right bottom).

In this work, we address this situation and extend the theory of cycle-consistency for partial overlap, for which we provide mathematical underpinnings. We then implement this theory to effectively handle partial overlap in the training data through a pseudo-mask, and introduce trainable cycle variations to obtain a richer learning signal, see Figure 1. Consequently, we can get more out of the training data, thus providing a stronger cycle-consistency learning signal. Our method is shown to be robust in more challenging settings, with lower overlap between cameras and fewer matches in the training data. It is especially effective for challenging scenes where few matches need to be found between many people. The additional information from partial cycle-consistency thus leads to substantial improvements, as shown in the experimental section.

Our contributions are as follows:

1. We extend the mathematical formulation of cycle-consistency to handle partial overlap, leading to a new formulation for partial cycle-consistency.
2. We use pseudo-masks to implement partial cycle-consistency and introduce several cycle variants, motivating how these translate to a richer self-supervision learning signal.
3. We experiment with cross camera matching on the challenging DIVOTrack dataset, and obtain systematic improvements. Our experiments highlight the merits of using a range of cycle variants, and indicate that our approach is especially effective in more challenging scenarios.

Section 2 covers related works on self-supervised feature learning. Section 3 summarizes our mathematical formulation and derivation of cycle-consistency with partial overlap. Section 4 details our self-supervised method. We discuss the experimental validation in Section 5 and conclude in Section 6.

2 Related work

We first address the general multi-view matching problem, and highlight its application areas. Section 2.2 summarizes supervised feature learning, whereas Section 2.3 details self-supervised alternatives.

2.1 Multi-View Matching

Many problems in computer vision can be framed as a multi-view matching problem. Examples include keypoint matching [16], video correspondence over time [12], shape matching [11], 3D human pose estimation [3], multi-object tracking (MOT) [17], re-identification (Re-ID) [23], and cross-camera matching (CCM) [8]. Cross-view multi-object tracking (CVMOT) combines CCM with a tracking algorithm [7,9]. The underlying problem is that there are more than two views of the same set of objects, and we want to find matches between the sets. For MOT, detections between two subsequent time frames are matched [22]. Instead, in CCM, detections from different camera views should be matched. One particular challenge is that the observations have significantly different viewing angles. Such invariancies should be handled effectively through a feature extraction network. Such networks can be trained using identity label supervision but obtaining consistent labels across cameras is labor-intensive [9], highlighting the need for good self-supervised alternatives.

2.2 Supervised Feature Learning

Supervised Re-ID methods [21,23] work well for CCM. With labels, feature representations from the same instance are metrically moved closer, while pushing apart feature representations from different instances. Other approaches such as

joint detection and Re-ID learning [9], or training specific matching networks [8] have been explored. Supervised methods for CCM typically degrade in performance when applied to unseen scenes, indicating issues with overfitting. Self-supervised cycle-consistency [7] has been shown to generalize better [9].

2.3 Self-Supervised Feature Learning

Self-supervised feature learning algorithms do not exploit labels. Rather, common large-scale self-supervised contrastive learning techniques [2] rely on data augmentation. We argue that the significant variations in object appearance across views cannot be adequately modeled through data augmentations, meaning that such approaches cannot achieve view-invariance. Clustering-based self-supervised techniques [5] are also not designed to deal with significant view-invariance. Another alternative is to learn self-supervised features through forcing dissimilarity between tracklets within cameras while encouraging association with tracklets across cameras [13].

Self-supervision with cycle-consistency is suitable for multi-camera systems because it enables learning to associate consistently between the object representations from different cameras and at different timesteps. Trainable cycles can be constructed as series of matchings that start and end at the same object. Each object should be matched back to itself as long as the object is visible in all views. If an object is matched back to a different one, a cycle-inconsistency has been found which then serves as a learning signal [12,20].

Given the feature representations of detections in two different views, a symmetric cycle between these two views can be constructed by combining two soft-maxed similarity matrices, matching back and forth. The feature network can then be trained by forcing this cycle to resemble the identity matrix with a loss [20]. This approach can be extended to transitive cycles between three views, which is sufficient to cover cycle-consistency between any number of views [7,11]. With little partial overlap in the training data, forcing cycles to resemble the full identity matrix [7,20] provides a diluted learning signal that trains many non-existent cycles without putting proper emphasis on the actual cycles that should be trained. It is therefore important to differentiate between possibly existing and absent cycles in each batch. To this end, we focus on partial cycles that can exist despite a lack of overlap between pairs of views. A work that was developed in parallel to ours [6] has also found improvements with a partial masking strategy. Our work confirms their observations that considering partial overlap improves matching performance. In addition, we provide a rigid mathematical underpinning, introduce more cycle variations, and trace back improvements to characteristics of the scene including the amount of overlap between views.

Learning with cycle-consistency is not exclusive to CCM. Cycles between detections at different timesteps can be employed to train a self-supervised feature extractor for MOT [1], and cycles between image patches or video frames can serve to learn correspondence features at the image level [4,12,19]. This highlights the importance of a rigid mathematical derivation of partial cycle-consistency in a self-supervised loss.

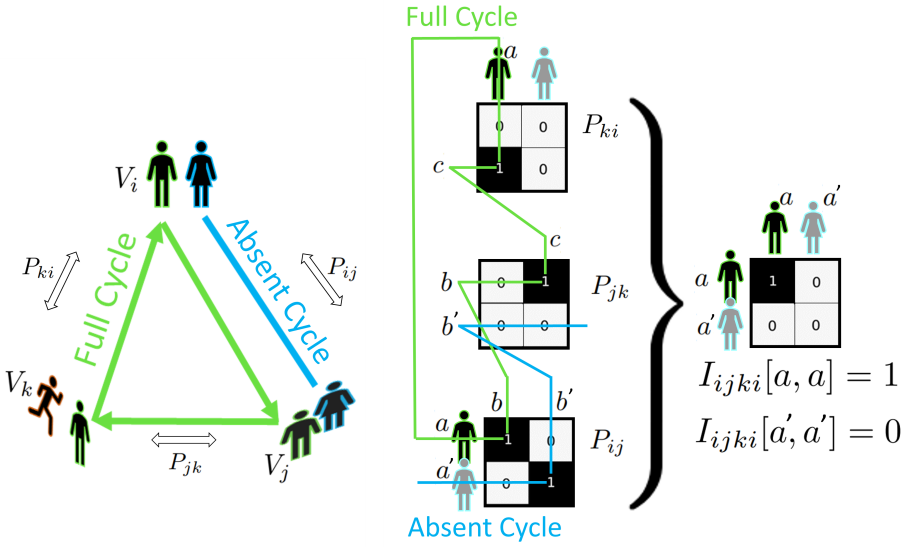

(a) Partial cycle-Consitency: Multiple views with partial overlap. Only the green person corresponds to an existing cycle.

(b) Interpretation of Equation 5. $I_{ijki}[a, a] = 1$ because a is matched to b, matched to c which is then matched back to a. The same does not hold for a', so this cycle is absent.

Fig. 2: Partial cycle-consistency and the explicit identification of existing and absent cycles between multiple views visualized.

3 Partial Cycle-Consistency Analysis

We summarize the main contributions from our theoretical extension of partial cycle-consistency, which appears in full in the supplementary materials [18]. Given are pairwise similarities $S_{ij} \in \mathbb{R}^{n_i \times n_j}\ \forall i, j$ between the views V_i, V_j, that contain n_i, n_j bounding boxes. Partial multi-view matching aims to obtain the optimal partial matching matrices $P_{ij} \in \{0, 1\}^{n_i \times n_j}\ \forall i, j$, given the S_{ij} that are partially cycle-consistent with each other. See also Figure 2a. Partial cycle-consistency implies that, among others, matching from view V_i to view V_j and then to view V_k should be a subset of the direct matching between V_i and V_k. We make this subset relation explicit, pinpointing which matches get lost through view V_j by inspecting the pairwise matches, proving equivalence to the original definition. We then prove that partial cycle-consistency in general only implies the most usable form of cycle-consistency for self-supervision, where matches are combined into full cycles that start and end in the same view and should thus be a subset of the identity matrix. This usable form of partial cycle-consistency is also made explicit. Based on this insight, in Section 4, we construct subsets of the identity matrix during training to serve as pseudo-masks, improving the

training process with partially overlapping views. Our explicit cycle-consistency proposition is:

Proposition 1 (Explicit partial cycle-consistency).
If a multi-view matching $\{P_{ij}\}_{\forall i,j}$ is partially cycle-consistent, it holds that:

$$P_{ii} = I_{n_i \times n_i} \quad \forall i \in \{1, \dots, N\}, \tag{1}$$

$$P_{ij}P_{ji} = I_{iji} \quad \forall i, j \in \{1, \dots, N\}, \tag{2}$$

$$P_{ij}P_{jk}P_{ki} = I_{ijki} \quad \forall i, j, k \in \{1, \dots, N\}, \tag{3}$$

where $I_{iji} \subseteq I_{n_i \times n_i}$ is the identity map from view i back to itself, filtering out matches that are not seen in view V_j:

$$I_{iji}[a, c] = \begin{cases} 1 & \text{if } a = c \ \& \ \exists b \text{ s.t. } P_{ij}[a, b] = 1. \\ 0 & \text{else,} \end{cases} \tag{4}$$

and where $I_{ijki} \subseteq I_{n_i \times n_i}$ is the identity mapping from view i back to itself, filtering out all matches that are not seen in views V_j and V_k:

$$I_{ijki}[a, d] = \begin{cases} 1 & \text{if } a = d \ \& \ \exists b, c \text{ s.t. } P_{ij}[a, b] = P_{jk}[b, c] = P_{ki}[c, d] = 1. \\ 0 & \text{else.} \end{cases} \tag{5}$$

The notation $X[\cdot, \cdot]$ is used for indexing a matrix X.

The intuition behind Equation 5 can be best understood through the visualization in Figure 2b. Here, $I_{ijki}[a', a'] = 0$ because there is a detection of a' absent in view V_k. The proofs can be found in the Appendix.

4 Self-Supervision with Partial Cycle-Consistency

The theory of cycle-consistency and its relation to partial overlap can be translated into a self-supervised feature network training strategy. The main challenges are to determine which cycles to train, which loss to use, and how to implement the findings from Proposition 1 to handle partial overlap. Section 4.1 explores what cycles to train and how to construct them. Section 4.2 explores how to obtain partial overlap masks for the cycles that approximate the $I_{iji}, I_{ijki} \subseteq I_{n_i \times n_i}$ from Proposition 1. It also explores how these masks can be incorporated in a loss to deal with partial overlap during training.

4.1 Trainable Cycle Variations

Given are the pairwise similarities S_{ij} between all view pairs, obtained from the feature extractor ϕ that we wish to train. The idea is to combine softmax matchings of the S_{ij} into cycles, similar to Equations 2 and 3. For this we use the temperature-adaptive row-wise softmax f_τ [20] on a similarity matrix S to

perform a soft row-wise partial matching. This function has the differentiability needed to train a feature network and the flexibility to make non-matches for low similarity values. We get:

$$f_\tau(S[a,b]) = \frac{\exp(\tau S[a,b])}{\sum_{b'} \exp(\tau S[a,b'])}, \tag{6}$$

where the notation $S[\cdot,\cdot]$ is used for matrix indexing. The temperature τ depends on the size of S as in [20].

Pairwise cycles. The pairwise cycles need to be constructed from just $S_{ij} = S_{ji}^T$. To this end, we take:

$$A_{ij} = f_\tau(S_{ij}), \quad A_{ji} = f_\tau, \quad (S_{ij}^T), A_{iji} = A_{ij}A_{ji}. \tag{7}$$

The cycle A_{iji} [20] represents a trainable variant of the pairwise cycle $P_{ij}P_{ji}$ from Equation 2, and so a learning signal is obtained by forcing it to resemble I_{iji}. Note that the A_{ij} and A_{ji} differ because they match the rows and columns of S_{ij}, respectively. This is important because the loss then forces these different soft matchings to be consistent with each other, modelling the partial cycle-consistency constraint in Equation 2. The loss will be the same for A_{iji} and $A_{iji}^T = A_{ji}^T A_{ij}^T$, so just Equation 7 suffices.

Triplewise cycles. The triplewise cycles are constructed from S_{ij}, S_{jk} and S_{ki}, and should resemble $P_{ij}P_{jk}P_{ki}$ from Equation 3. The authors in [6] propose:

$$A_{ijki}^0 = A_{ij}A_{jk}A_{ki}, \tag{8}$$

while in [7], the similarities are combined first such that:

$$S_{ijk} = S_{ij}S_{jk}, \quad A_{ijk} = f_\tau(S_{ijk}), \tag{9}$$

with which the triplewise cycle is created as:

$$A_{ijki}^1 = A_{ijk}A_{kji}. \tag{10}$$

We discovered that using multiple triplewise cycle constructions in the training improves the results. Each of the constructed cycles exposes a different inconsistency in the extracted features, such that a combination of cycles provides a robust training signal. We propose to use the following four triplewise cycles:

$$A_{ijki}^0 = A_{ij}A_{jk}A_{ki}, \tag{11}$$

$$A_{ijki}^1 = A_{ijk}A_{kji}, \tag{12}$$

$$A_{ijki}^2 = A_{ijk}A_{ki}, \tag{13}$$

$$A_{ijki}^3 = A_{ijk}A_{kij}A_{jki}. \tag{14}$$

The cycles from Equation 12-14 are also visualized in Figure 1 as the three blue swirls. In the following, A_{ijki} can be used to refer to any of the four triplewise cycles in Equations 11- 14, and additionally A_{iji} when assuming $j = k$. The symmetric property of the loss makes the transposed versions of Equations 11 - 14 redundant.

4.2 Masked Partial Cycle-Consistency Loss

The A_{ijki} can be directly trained to resemble the identity matrix I_{ii}, by training each diagonal element in A_{ijki} to be a margin m greater than their corresponding maximum row and column values, similar to the triplet loss [20,7]. This is achieved through:

$$L_m(A_{ijki}) = \sum_{i=1}^{n_i} \text{relu}(\max_{b \neq a}(A_{ijki}[a,b]) - A_{ijki}[a,a] + m). \tag{15}$$

The following loss enforces this margin over both the rows and columns:

$$\mathcal{L}_m(A_{ijki}) = \frac{1}{2}(L_m(A_{ijki}) + L_m(A_{ijki}^T)). \tag{16}$$

This loss, however, does not distinguish between absent and existing cycles that occur with partial overlap. Note that the ground truth I_{ijki} are masks (or subsets) of the I_{ii} that exactly filter out such absent cycles, while keeping the existing cycles, according to Equation 5 and visualized in Figure 2b. In this figure, detections of the blue person form an absent cycle because the pairwise matches are not connected. The I_{ijki} are constructed based on the ground truth matches P_{ij}. We therefore propose to construct pseudo-masks $\widetilde{I}_{ijki}$ from pseudo-matches $\widetilde{P}_{ij}$ that are available during self-supervised training. For this we use:

$$\widetilde{P}_{ij} = \begin{cases} [f_\tau(S_{ij}) \ > 0.5] & \text{if } |V_i| < |V_j|, \\ \left[f_\tau(S_{ij}^T)^T > 0.5\right] & \text{if } |V_j| < |V_i|, \end{cases} \tag{17}$$

where the Iverson bracket $[Predicate(X)]$ binarizes matrix X, with elements equal to 1 for which the predicate is true, and 0 otherwise. In $\widetilde{P}_{ij}$, each element in a view with fewer elements can be matched to at most one element in the other view, as desired for a partial matching. We construct the pseudo-masks as:

$$\widetilde{I}_{ijki}[a,a] = \begin{cases} 1 & \text{if } \exists b,c \text{ s.t. } \widetilde{P}_{ij}[a,b] = \ \widetilde{P}_{jk}[b,c] = \widetilde{P}_{ki}[c,a] = 1. \\ 0 & \text{else.} \end{cases} \tag{18}$$

$\widetilde{I}_{ijki}$ is invariant to the order in the i,j,k sequence, and independent of the cycle variant for which it is used as a mask. Equation 18 can be vectorized as:

$$\widetilde{I}_{ijki} = \left[\widetilde{P}_{ij}\widetilde{P}_{jk}\widetilde{P}_{ki} \odot I_{ii} \geq 1\right]. \tag{19}$$

Our masked partial cycle-consistency loss extends the loss from Equation 16 with the pseudo-masks $\widetilde{I}_{ijki}$, for which only the diagonal elements of predicted existing cycles are 1. The absent cycles have diagonal elements of 0. The loss uses two different margins $m_+ > m_\emptyset > 0$, where m_+ is used for cycles that are predicted to exist with $\widetilde{I}_{ijki}$, and $m_\emptyset$ is used for the cycles predicted to be absent:

$$\mathcal{L}_{explicit} = \frac{1}{2}(\mathcal{L}_{m_+}(\widetilde{I}_{ijki} \odot A_{ijki}) + \mathcal{L}_{m_\emptyset}((I_{ii} - \widetilde{I}_{ijki}) \odot A_{ijki})). \tag{20}$$

5 Results and Experiments

We demonstrate the merits of a stronger self-supervised training signal from the addition of our cycle variations and partial cycle-consistency mask. We introduce the training setting, before detailing our quantitative and qualitative results.

Dataset and metrics. DIVOTrack [9] is a large and varied dataset of time-aligned overlapping videos with consistently labeled people across cameras. The publicly available data contains 54k frames divided over three overlapping cameras. There are 10 different scenes, split equally over the train and test set, containing some of the same but mostly different people. Our self-supervised feature network trains without the labels. We report the cross-camera matching precision, recall and F1 score [8] on the test set, averaged over five training runs. Ablations on overlap and cycle variants are computed over the first three runs. The F1 standard deviation is reported as a measure of variability between runs.

Implementation details. Our contributions extend [7], the state-of-the-art in self-supervised training. Our cycle variations from Equations 11-14 are used instead of theirs, with attention to the specific view pairs and triples. This provides a diverse set of cycles to capture different cycle-inconsistencies. Methods without masking use the loss from Equation 16. Our partial masking strategy instead first constructs pseudo-masks with Equation 18 and uses these in our explicit partial masking loss from Equation 20, with $m_+ = 0.7$ and $m_\emptyset = 0.3$. We use the same training setup as [7] for fair comparison. Specifically, we use annotated bounding boxes without identity labels to extract features to train a ResNet-50 [10] for 10 epochs with an Adam optimizer with learning rate $1e-5$. Matching inference uses the Hungarian algorithm between all view pairs, using the optimal partial overlap inference parameter for each model which determines non-matches.

Time-divergent scene sampling. Detections from multiple cameras at two timesteps are used in a batch such that cycles are constructed and trained between the pairs and triples for $2C$ views of the same scene, C the number of cameras [6,7]. Time-divergent scene sampling gradually increases the interval Δt between timesteps during training, with Δt equal to the current epoch number. It also uses fractional sampling to obtain a balanced batch order, such that the local distribution of scenes resembles the average global distribution of scenes.

5.1 Main Results

We show the effectiveness of our cycle variations and partial masking as additions to the existing self-supervised SOTA [7] in Table 1. We report the results both with and without time-divergent scene sampling, as this approach simply makes the data input richer, improving performance regardless of the cycle-consistency method used. We find that combining cycle variations, partial masking and Time Divergent Scene Sampling boosts the F1 matchings score of the previous SOTA by 4.3 percentage points, and that this combination is also the most consistent of all approaches. A Resnet pretrained on ImageNet obtains a matching score of 16.8 on the test data, and a supervised SOTA Re-ID model [23] with an optimized network architecture and hard negative mining obtains a matching

score of 82.28 for comparison. This illustrates the strength of self-supervised cycle-consistency in general, showcasing its ability to significantly improve the feature quality of the ResNet. It also shows that our unoptimized self-supervised method is not to far from an optimized supervised baseline.

Model	**Standard**			**Time-Div. Scene Sampling**		
	Precision	Recall	F1	Precision	Recall	F1
MvMHAT [7]	66.3	60.1	63.1±1.7	68.0	62.8	65.3±1.3
Cycle variations (CV)	68.8	**61.1**	64.7±1.9	70.4	62.3	66.1±1.4
CV + Partial masking	**71.0**	61.0	**65.6±1.1**	**71.7**	**63.6**	**67.4±0.9**

Table 1: Cycle variations and partial masking together improve the overall matching performance by 2.5-2.1 percentage points. Every method benefits from time-divergent scene sampling, and combining everything boosts the previous SOTA by 4.3 percentage points, also improving stability.

Results per scene. The 10 scenes in the train and test data provide different challenges. During training, scenes with little overlap provide a worse learning signal for the overall model. During testing, scenes that require matchings between many people are significantly more challenging. Insights into the specific overlap and average number of people per scene during training and testing are provided in the supplementary materials [18]. The scenes Ground, Side and Shop contain the highest number of people, around 24-32 per frame on average, and can thus be considered as the most challenging test set scenes to match correctly. Table 2 reports the matching results per scene. Our methods outperform [7] on every test set, with the largest (relative) gains on Ground, Side and Shop, with 9.1, 5.6 and 4.7 percentage points, respectively, highlighting the improved expressiveness of our feature network.

Methods	**Gate2**	**Square**	**Moving**	**Circle**	**Gate1**
MvMHAT [7]	88.1	73.3	73.1	67.4	67.2
Ours w\o Masking	**88.3(+0.2)**	**74.9(+1.6)**	74.9(+1.8)	68.7(+1.3)	69.6(+2.4)
Ours	**88.3(+0.2)**	**74.9(+1.6)**	**76.2(+3.1)**	**69.9(+2.5)**	**70.4(+3.2)**
Methods	**Floor**	**Park**	**Ground**	**Side**	**Shop**
MvMHAT [7]	64.7	58.2	56.9	56.0	42.1
Ours w\o Masking	65.2(+0.5)	58.4(+0.2)	64.5(+7.6)	58.9(+2.9)	45.5(+3.4)
Ours	**66.8(+2.1)**	**60.4(+2.2)**	**66.0(+9.1)**	**61.6(+5.6)**	**46.8(+4.7)**

Table 2: Results per scene. Our methods improve the average F1 score on every scene. Crowded test scenes like **Ground**, **Side** and **Shop** benefit most.

Partial overlap experiments. We experiment with artificially reducing the field of view in the training data by 20-40%. We implement this by reducing the actual width of each camera view starting from the right, throwing away the bounding boxes outside this reduced field of view. We train on these reduced overlap datasets and evaluate on the full test data to measure the robustness for each method, because self-supervision through cycle-consistency learns from overlap. An overlap analysis for the original and reduced datasets is provided in Table 3, and the evaluation results when training with the reduced data are shown in Table 4. We observe that our method is robust and contributes to the performance in harder training scenarios.

Jaccard Index	**Full Train|Test**	**80% Train Overlap**	**60% Train Overlap**
Two Cameras	0.40|0.38	0.37	0.29
Three Cameras	0.26|0.23	0.24	0.15
Num People	18.4|19.4	16.5	14.0

Table 3: The original train dataset has an average of 40% IoU between any two cameras, 26% people visible in all three cameras, and 18.4 unique people per frame. We reduce the FOV to simulate harder train data with less overlap.

	Full Train	**80% Train Overlap**	**60% Train Overlap**
Methods		**test set F1 score**	
MvMHAT [7]	63.1±1.7	60.6±1.6	55.0±2.3
Ours w\o Masking	66.1±1.4	63.0±1.9	56.5±2.3
Ours	**67.4±0.9**	**63.8 ± 1.2**	**57.9 ± 1.5**

Table 4: Our methods consistently improve performance, even with sparser training data that is reduced in partial overlap.

Cycle variations ablation. Our cycle variations use Equations 11- 14 to construct multiple trainable cycles to obtain a richer learning signal. We perform an ablation study on the effectiveness of each cycle, with and without the masking, in Table 5. We find that the $A_{ijk}A_{ki}$ cycle (Equation 13) performs well, both on its own and when combined with other variations. We take the best performing cycle combinations and combine them with partial masking. We observe that using multiple cycle variations works especially well in the presence of masking, showing that these methods partly complement each other.

5.2 Qualitative Results

Figure 3 illustrates the contribution of the various cycles and pseudo-mask during training. In this specific example, it can be seen how the varied cycle constructions are cycle-inconsistent in different ways. Consequently, a robust learning

$A_{ijk}A_{kji}$ Eq 12 [7]	$A_{ijk}A_{ki}$ Eq 13 [Ours]	$A_{ijk}A_{kij}A_{jki}$ Eq 14 [Ours]	$A_{ij}A_{jk}A_{ki}$ Eq 11 [6]	**w\o Masking**	**with Masking**
✓				65.1 ± 0.9	-
	✓			**66.4 ± 1.0**	66.2 ± 1.5
		✓		65.6 ± 1.8	-
			✓	57.7 ± 1.5	-
✓	✓			65.6 ± 1.5	66.7 ± 0.9
✓	✓	✓		66.2 ± 1.2	66.9 ± 0.7
✓	✓	✓	✓	66.3 ± 1.0	**67.2 ± 1.1**

Table 5: Ablation of the cycle variations. Our $A_{ijk}A_{ki}$ cycle works well individually, and in combination with other cycle variations. Combining more cycle variations works especially well when also combined with partial masking.

signal is obtained from combining all cycle variants. The figure also shows the pseudo-mask I_{ijki} that is constructed for this batch, where the existing cycles are correctly found with the exception of a severely occluded one in the top left. The low value of 0.36 on the diagonal of the dark blue cycle provides a strong self-supervised learning signal due to the masking, such that the model will learn similar features for the different views of the person in pink.
Figure 4 provides insight into the test set matching performance of our model compared to [7]. It shows how our model effectively finds the pairwise matches at test time in a crowded scene. Note the difficulty of the matching problem, and how our method has significantly fewer false positive matches. The figure also demonstrates that our method is able to match significantly different representations of the same person across cameras, based on subtle clothing details.

6 Conclusion

We have extended the mathematical formulation of cycle-consistency to partial overlaps between views. We have leveraged these insights to develop a self-supervised training setting that employs various newly introduced cycle variants and a pseudo-masking approach to steer the loss function. These cycle variants expose different cycle-inconsistencies, ensuring that the self-supervised learning signal is more diverse and therefore stronger. We also presented a time divergent batch sampling approach for self-supervised cycle-consistency. Our methods combined, improve the cross-camera matching performance of the current self-supervised state-of-the-art on the challenging DIVOTrack benchmark by 4.3 percentage points overall, and by 4.7-9.1 percentage points for the most challenging scenes.

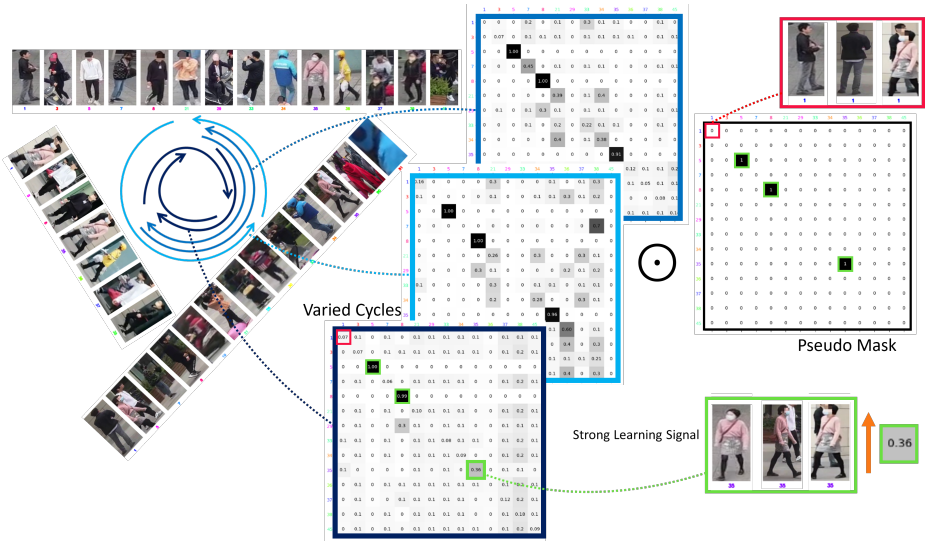

Fig. 3: Each of the blue swirls, representing Equations 12-14, constructs a cycle matrix with various cycle-inconsistencies. Partial overlap requires that only some of the diagonal elements are trained as cycles. The pseudo-mask correctly finds the existing cycles, except for a heavily occluded one. A strong learning signal is obtained from one of the diagonals of the dark blue cycle.

Our method is effective in other multi-camera downstream tasks such as Re-ID and cross-view multi-object tracking. One limitation of self-supervision with cycle-consistency is its dependence on bounding boxes in the training data. Detections from an untrained detector could be used to train with instead, but this would likely degrade performance. Another area for improvement is to take location and relative distances into account both during training and testing, as this provides informative identity information.

Self-supervision through cycle-consistency is applicable to many more settings than just learning view-invariant object features. We believe the techniques introduced in this paper also benefit works that use cycle-consistency to learn image, patch, or keypoint features from videos or overlapping views.

References

1. Bastani, F., He, S., Madden, S.: Self-supervised multi-object tracking with cross-input consistency. Advances in Neural Information Processing Systems **34**, 13695–13706 (2021)
2. Chen, T., Kornblith, S., Norouzi, M., Hinton, G.: A simple framework for contrastive learning of visual representations. In: International conference on machine learning. pp. 1597–1607. PMLR (2020)

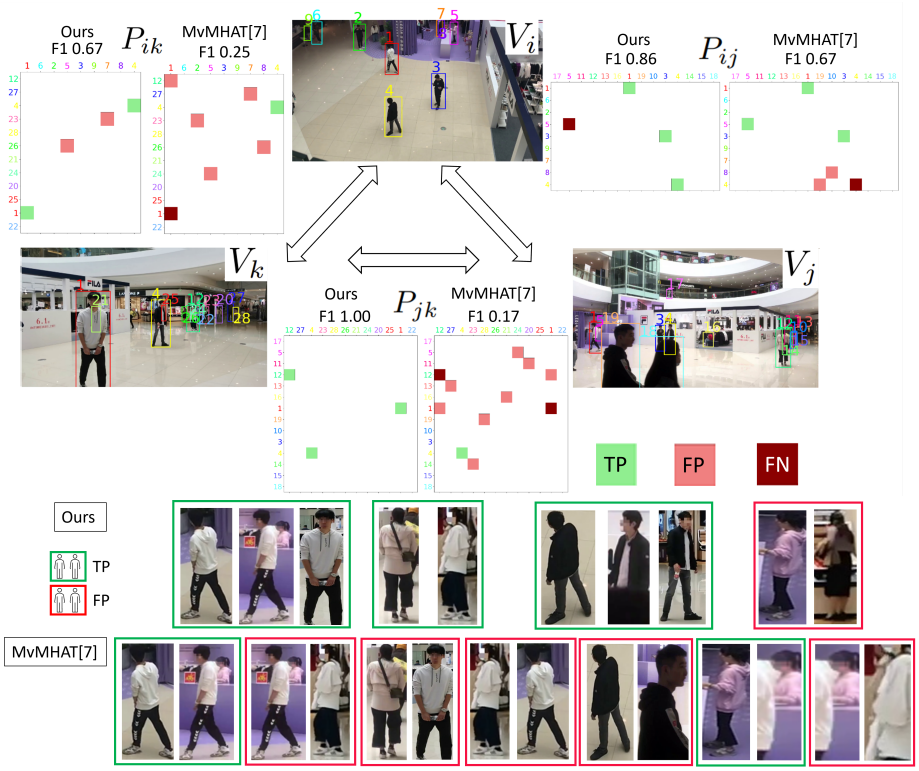

Fig. 4: Visualized matchings for a difficult frame in the test set. Our model is able to match with significantly fewer false positives. The matches found with our method are based on subtle clothing details, and have been correctly found in the presence of significant view angle differences and occlusion.

3. Dong, J., Jiang, W., Huang, Q., Bao, H., Zhou, X.: Fast and robust multi-person 3d pose estimation from multiple views. In: Proceedings of the IEEE/CVF conference on computer vision and pattern recognition. pp. 7792–7801 (2019)
4. Dwibedi, D., Aytar, Y., Tompson, J., Sermanet, P., Zisserman, A.: Temporal cycle-consistency learning. In: Proceedings of the IEEE/CVF conference on computer vision and pattern recognition. pp. 1801–1810 (2019)
5. Fan, H., Zheng, L., Yan, C., Yang, Y.: Unsupervised person re-identification: Clustering and fine-tuning. ACM Transactions on Multimedia Computing, Communications, and Applications (TOMM) **14**(4), 1–18 (2018)
6. Feng, W., Wang, F., Han, R., Qian, Z., Wang, S.: Unveiling the power of self-supervision for multi-view multi-human association and tracking. arXiv preprint arXiv:2401.17617 (2024)
7. Gan, Y., Han, R., Yin, L., Feng, W., Wang, S.: Self-supervised multi-view multi-human association and tracking. In: Proceedings of the 29th ACM International Conference on Multimedia. pp. 282–290 (2021)

8. Han, R., Wang, Y., Yan, H., Feng, W., Wang, S.: Multi-view multi-human association with deep assignment network. IEEE Transactions on Image Processing **31**, 1830–1840 (2022)
9. Hao, S., Liu, P., Zhan, Y., Jin, K., Liu, Z., Song, M., Hwang, J.N., Wang, G.: Divotrack: A novel dataset and baseline method for cross-view multi-object tracking in diverse open scenes. International Journal of Computer Vision pp. 1–16 (2023)
10. He, K., Zhang, X., Ren, S., Sun, J.: Deep residual learning for image recognition. In: Proceedings of the IEEE conference on computer vision and pattern recognition. pp. 770–778 (2016)
11. Huang, Q.X., Guibas, L.: Consistent shape maps via semidefinite programming. Computer graphics forum **32**(5), 177–186 (2013)
12. Jabri, A., Owens, A., Efros, A.: Space-time correspondence as a contrastive random walk. Advances in neural information processing systems **33**, 19545–19560 (2020)
13. Li, M., Zhu, X., Gong, S.: Unsupervised tracklet person re-identification. IEEE transactions on pattern analysis and machine intelligence **42**(7), 1770–1782 (2019)
14. Loy, C.C., Xiang, T., Gong, S.: Time-delayed correlation analysis for multi-camera activity understanding. International Journal of Computer Vision **90**, 106–129 (2010)
15. Ristani, E., Tomasi, C.: Features for multi-target multi-camera tracking and re-identification. In: Proceedings of the IEEE conference on computer vision and pattern recognition. pp. 6036–6046 (2018)
16. Sarlin, P.E., DeTone, D., Malisiewicz, T., Rabinovich, A.: Superglue: Learning feature matching with graph neural networks. In: Proceedings of the IEEE/CVF conference on computer vision and pattern recognition. pp. 4938–4947 (2020)
17. Sun, S., Akhtar, N., Song, H., Mian, A., Shah, M.: Deep affinity network for multiple object tracking. IEEE transactions on pattern analysis and machine intelligence **43**(1), 104–119 (2019)
18. Taggenbrock, F.: Supplementary materials for self-supervised partial cycle-consistency for multi-view matching. `https://github.com/FedorTaggenbrock/Self-Supervised-Partial-Cycle-Consistency` (2024)
19. Wang, X., Jabri, A., Efros, A.A.: Learning correspondence from the cycle-consistency of time. In: Proceedings of the IEEE/CVF Conference on Computer Vision and Pattern Recognition. pp. 2566–2576 (2019)
20. Wang, Z., Zhang, J., Zheng, L., Liu, Y., Sun, Y., Li, Y., Wang, S.: Cycas: Self-supervised cycle association for learning re-identifiable descriptions. In: Computer Vision–ECCV 2020: 16th European Conference, Glasgow, UK, August 23–28, 2020, Proceedings, Part XI 16. pp. 72–88. Springer (2020)
21. Wieczorek, M., Rychalska, B., Dąbrowski, J.: On the unreasonable effectiveness of centroids in image retrieval. In: Neural Information Processing: 28th International Conference, ICONIP 2021, Sanur, Bali, Indonesia, December 8–12, 2021, Proceedings, Part IV 28. pp. 212–223. Springer (2021)
22. Wojke, N., Bewley, A., Paulus, D.: Simple online and realtime tracking with a deep association metric. In: 2017 IEEE international conference on image processing (ICIP). pp. 3645–3649. IEEE (2017)
23. Ye, M., Shen, J., Lin, G., Xiang, T., Shao, L., Hoi, S.C.: Deep learning for person re-identification: A survey and outlook. IEEE transactions on pattern analysis and machine intelligence **44**(6), 2872–2893 (2021)
24. Zhao, J., Han, R., Gan, Y., Wan, L., Feng, W., Wang, S.: Human identification and interaction detection in cross-view multi-person videos with wearable cameras. In: Proceedings of the 28th ACM International Conference on Multimedia. pp. 2608–2616 (2020)